




# Molecularly imprinted photonic hydrogel sensor for optical detection of L-histidine

Qianshan Chen<sup>1</sup> · Wenhui Shi<sup>1</sup> · Meifang Cheng<sup>1</sup> · Shuzhen Liao<sup>2</sup> · Jun Zhou<sup>1</sup> · Zhaoyang Wu<sup>1</sup> 

Received: 30 July 2018 / Accepted: 31 October 2018 / Published online: 21 November 2018  
© Springer-Verlag GmbH Austria, part of Springer Nature 2018

## Abstract

A molecularly imprinted photonic hydrogel (MIPH) is described for the optical determination of L-histidine (L-His). The inverse opal structure of MIPH was obtained by placing silica particles (230 nm) in molecularly imprinted polymer on a glass slide. After being fully etched by hydrofluoric acid, this inverse opal structure brings about a high specific surface and plentiful binding sites for L-His. If L-His is absorbed by the modified MIPH, its average effective refraction coefficient is increased. This causes the Bragg diffraction peak to be red-shifted by about 34 nm as the concentration of L-His increases from 0 to 100 nM. Much smaller diffraction peak shifts are obtained for other amino acids. The detection limit of this method is 10 pM. The response time towards L-His is as short as 60 s. In addition, the sensor can be recovered by treatment with 0.1 M acetic acid/methanol. It was applied to the determination of L-His in drinks sample.

**Keywords** Photonic crystal array · Inverse opal structure · Bragg diffraction peak · Nanoporous materials · Reflection spectrum · UV curing · Hydrogen bonding · Stöber method

## Introduction

L-Histidine (L-His) is an important building block for brain peptides and of muscle proteins [1, 2]. It can form a Zn-[His]<sub>2</sub> complex after integrating with Zn<sup>2+</sup>, which can decrease toxicity of necrotic cell and increase cell proliferation of human keratinocytes [3]. It has been reported that the under-expression or over-expression of L-His may cause many diseases, like Friedreich ataxia, Parkinson's disease, chronic kidney disease and psychological disorder [4]. Many analytical methods have been reported for the determination of L-His, such as capillary electrophoresis (CE) [5], high performance

liquid chromatography (HPLC) [6], fluorescence spectrometry [7–9], electrochemistry [10, 11] and mass spectrometry [12]. These methods have shown many advantages for detection of L-His, but they still suffer from drawbacks such as requirement of expensive and sophisticated instruments, complexity of separate analytical procedures, and so on. Therefore, it is of great significance to develop a rapid, selective and sensitive method to detect L-His.

Photonic crystals (PhCs) are made of periodic arrangements of materials with different dielectric constant, which can effectively control the direction of optical propagation due to the structure of the photonic band gap (PBG) [13–15]. Responsive hydrogel PhCs (RHPCs) has been recently developed by combining responsive hydrogel with PhCs. The RHPCs can make a specific response to the chemical or environmental stimulus and lead a shift of the Bragg diffraction peak, which can be detected by spectrometer. Some RHPCs have been reported for detecting various chemical stimuli, such as ionic strength and pH [16, 17], metal ions [18], glucose [19], stimulants [20] and enzymes [21]. Molecularly imprinted polymers (MIPs) is a kind of booming material with special molecular recognition function for target molecules [22], which has abundant binding sites and specific recognition nano-cavities [23–26]. Due to the high specificity for target molecules, the MIPs has been got widely used in multiple fields like analysis and separation

✉ Jun Zhou  
zhouj\_cn@163.com

✉ Zhaoyang Wu  
zywu@hnu.edu.cn

Shuzhen Liao  
liaoshuzhen835600@126.com

<sup>1</sup> State Key Laboratory of Chemo/Biosensing and Chemometrics, College of Chemistry and Chemical Engineering, Hunan University, Changsha 410082, People's Republic of China

<sup>2</sup> School of Chemistry and Chemical Engineering, Hunan Institute of Engineering, Xiangtan 411104, People's Republic of China

technology [27–30]. However, the sensing methods based on MIPs are usually appropriate for the target molecules with specific optical or electrical signals [31], which may profoundly limit its applications.

It is an interesting strategy to develop molecularly imprinted photonic hydrogel (MIPH) sensor by combining molecularly imprinted polymers with PhCs, which has the special selectivity of MIPs and the readable optical signal of PhCs at the same time [32]. Comparing with the conventional MIPs, this MIPH sensor has some advantages. (1) The ordered porous structure makes the sensor have superior performance because the MIPH has high specific surface area and efficient mass transportation. (2) There is no need to modify the target molecules with specific optical or electrical signals. The Bragg diffraction peak of MIPH will shift after combining with target molecules, this property can be used to optically determine analytes. Hu et al. reported a self-reporting recognition function by using both colloidal crystals and molecular imprinting techniques in the first time [33].

A novel MIPH sensor was developed for optical detection of L-His. The preparing process and response principle are shown in Fig. 1a. The highly-ordered silica PhCs template is first prepared by vertical self-assembly, the precursor solution (contains target molecules, function monomers and cross-linker) is injected into the PhCs template and then photopolymerized under UV light. After removing the silica particles and L-His molecules, the MIPH with inverse opal structure is finally obtained. L-His molecules can be reversibly bound to the specific sites in the MIPH, which can cause the change of the physicochemical properties of hydrogel and further produce a redshift in the diffraction peak. And the Fig. 1(b) shows that the nano-cavities binding reversibly with L-His by non-covalent interactions, and Fig. 1(c) shows the photograph of the measuring set-up. The MIPH have rich specific sites, which making the sensor is expected to be a potential alternative for the selective and sensitive detection of L-His molecules.

## Experimental

### Materials and reagents

L-Histidine, cysteine, glycine, lysine, tryptophan, Tyrosine, L-phenylalanine, methacrylic acid (MAA), ethylene glycol dimethyl acrylate (EGDMA), 2-hydroxy-2-methylpropiophenone (HMPP), tetraethyl orthosilicate (TEOS) were obtained from Sigma-Aldrich (St. Louis, MO USA, [www.sigmaaldrich.com](http://www.sigmaaldrich.com)). D-His and His were obtained from Adamas (Shanghai, China, [www.adamas-beta.com](http://www.adamas-beta.com)). All above chemicals were used as received without further purification. Anhydrous ethanol, anhydrous methanol, ammonium hydroxide, hydrofluoric acid, acetic acid and other chemicals were purchased from Sinopharm Chemical

Reagent Co., Ltd. with analytical grade (Shanghai, China, [www.sinoreagent.com](http://www.sinoreagent.com)). Poly(methyl methacrylate) (PMMA) slides (25.4 × 76.2 mm, 2 mm thick) and microscope slides (25.4 × 76.2 mm, 1 mm thick) were bought from local suppliers. Ultrapure water (18.2 MΩ cm) was used in all solutions.

Before the experiments, the microscope slides and beakers for growing PhCs were cleaned by immersing in a H<sub>2</sub>SO<sub>4</sub>/H<sub>2</sub>O<sub>2</sub> mixture (7:3, V/V) for 3 h at 80 °C, then rinsed three times with ultrapure water and dried by N<sub>2</sub> flow. The phosphate buffer of NaH<sub>2</sub>PO<sub>4</sub> and Na<sub>2</sub>HPO<sub>4</sub> (pH 7.6, 10 mM) was used for all measurements.

### Preparation of opal structure photonic crystals (PhCs)

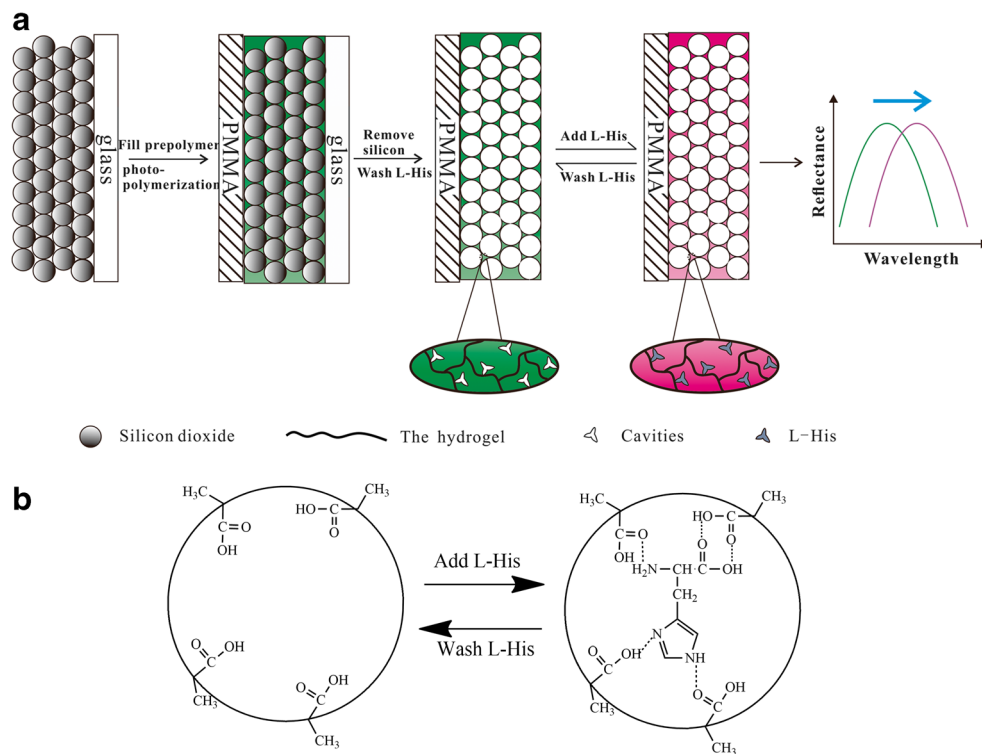
The PhCs of opal structure were prepared by using SiO<sub>2</sub> particles through vertical deposition technique. The highly homogeneous silica particles were formed by Stöber method [34]. First, 8.65 mL of TEOS and 150 mL of anhydrous ethanol were mixed in a 250 mL flask and stirring intensively with a magnetic beater, then slowly added 14 mL of ammonium hydroxide for reacting 10 h at room temperature. The SiO<sub>2</sub> particles were obtained by centrifugation at 8000 rpm and washed with water. The size of SiO<sub>2</sub> particles can be adjusted in a range of 150–400 nm by changing the concentrations of TEOS and ammonium hydroxide.

Then the SiO<sub>2</sub> particles were dispersed in ethanol (about 1% w/w) and stored in a 25 mL beaker. The cleaned microscope slide was put vertically into the beaker at 50 °C for 12 h, and the close packing PhCs film with bright green color was then formed on the microscope slide after volatilization of ethanol.

### Preparation of inverse opal structure molecularly imprinted photonic hydrogel (MIPH)

The MIPH was prepared by the following steps. L-His (7.8 mg, 0.05 mmol), MAA (59.4 μL, 0.7 mmol) and EGDMA (28.6 μL, 0.15 mmol) were fully mixed in a mixture of ultrapure water (50 μL) and anhydrous methanol (100 μL). The HMPP of 5 μL was then added, and the mixture was thoroughly blended in an ultrasonic bath for 5 min and degassed with N<sub>2</sub> for another 5 min. The microscope slide with PhCs film was covered by a PMMA slide to form a sandwich structure, and the above mixture was infiltrated into the space between the two slides by capillary forces. While the templates became transparent, indicating the voids of PhCs have been completed filled. After this, the mixture was photo-polymerized under the UV light (50 W) at 365 nm for 20 min, and then the sandwich structure was immersed in 1% hydrofluoric acid for 2 h to separate the PMMA slide from microscope slide. The hydrogel film with inverse opal photonic crystals (IOPCs) structure was finally obtained on the PMMA slide after the silica particles were fully etched. Then, the MIPH was rinsed by 0.1 M acetic acid/methanol to remove L-His. Next, the hydrogel film was

**Fig. 1** **a** Schematic illustration of the preparing process of molecularly imprinted photonic hydrogel and the diffraction peak of the MIPH changes to red-shift after combining with L-His. **b** The nano-cavities binding reversibly with L-His by non-covalent interactions. **c** The photograph of the measuring set-up



rinsed by the phosphate buffer and stored in phosphate buffer for use. To perform a control experiment, the non-imprinted photonic hydrogel (NIPH) was formed with the same procedure only without addition of L-His in above mixture.

### Detection of L-His

For the absorption detection, MIPH (20 mg) was immersed in 10 mL L-His solutions at various concentrations from 20 to 100  $\mu$ M for 3 h at room temperature. Then, the free concentration of L-His was determined by UV/Vis spectrometer. The amount of adsorption was calculated by subtracting the free concentrations from the initial concentrations.

The drinks sample was bought from local market and processed as follows. 2 mL of sample was filtered by a 0.22  $\mu$ m filter membrane, and then 1 mL of filtrate was diluted for 100-fold with phosphate buffer (pH 7.6, 10 mM) for analysis. Then, the L-His was added to configure as a series of concentration gradients from 10 pM - 100 nM. No further complex procedures were needed in the sample preparation.

### Characterization

The SiO<sub>2</sub> particles were collected by a centrifuging apparatus (Neofuge 23R, Heal Force, Shanghai). Surface morphology of the PhCs was observed by Scanning electron microscope

(Sigma HD, Carl Zeiss AG, German). The surface structure of MIPH was observed by Atomic force microscopy (Bioscope system, Bruker, America) and Scanning electron microscope (Sigma HD, Carl Zeiss AG, German). The photopolymerization was implemented under UV light (Sciencz 03-II, Sciencz, Ningbo). The UV/Vis spectrometer (UV 1800, Shimadzu, Japan) was used for investigating the concentration of L-His solution. The sensing property to MIPH was measured by immersing them in the phosphate buffer solutions containing a series of concentrations of L-His molecules. The shifts of Bragg diffraction wavelength of MIPH were recorded by a fiber-optic spectrometer (NOVA, IdeoOptics, Shanghai) which was mounted on a microscope (ECLIPSE 50iPOL, Nikon, Japan) in vertical direction.

## Results and discussion

### Fabrication and characterization of the L-His imprint (MIPH)

The close packed PhCs array was prepared with the mono-dispersed silica nano-spheres, and the inverse opal MIPH was obtained after a silica etching process. Figure 2a shows the SEM image of SiO<sub>2</sub> PhCs template, and the diameters of SiO<sub>2</sub> are about 230 (±3) nm. And the obtained MIPH film has the nano-cavities arrange orderliness, and the diameter of nano-

cavities without water are about 170 (±5) nm (Fig. 2b and c). On the one hand, the ordered porous inverse opal structure of the MIPH can produce excellent optical signals. On the other hand, this specific structure can make the target molecules easily to combine with the binding sites due to the high specific surface areas in MIPH film, and make this sensor respond rapidly and sensitively.

The diffraction light of the MIPH with periodic structure conforms to the Bragg's law:

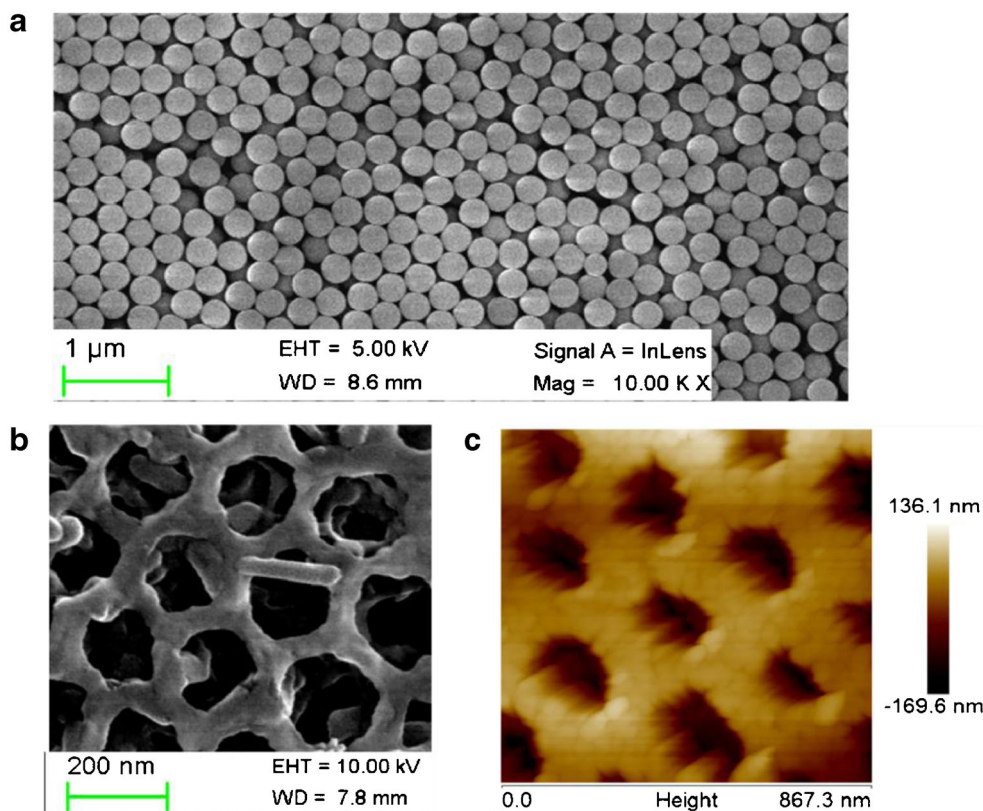
$$\lambda_{\max} = 2d_h n_{\text{eff}} \sin\theta \quad (1)$$

In which  $\lambda_{\max}$  is the maximum diffraction wavelength of MIPH,  $d_h$  is the crystallographic plane spacing between the two adjacent layers in the vertical direction (for this close packed face centered cubic structure,  $d_h = (2/3)^{1/2}D$ ,  $D$  is the sphere diameter of the macro-porous).  $\theta$  is the angle of incidence, and it is chosen as 90° (normal incidence) here. And  $n_{\text{eff}}$  is the average effective refractive coefficient of imprinted hydrogel film ( $n_c$ ) and water ( $n_0$ ). The value of  $n_{\text{eff}}$  follows the below equation:

$$n_{\text{eff}}^2 = f n_0^2 + (1-f) n_c^2 \quad (2)$$

Where  $f$  is the percentage of the volume of the macro-porous in the entire hydrogel space, and the value of  $f$  is 0.74 in this face centered cubic structure. The  $\lambda_{\max}$  was controlled by choosing the suitable size of silica particles. The

**Fig. 2** **a** The SEM of PhCs array on grass. **b** The SEM of inverse opal structure of MIPH. **c** The AFM image of MIPH film



structural color of MIPH was green in the blank phosphate buffer (pH 7.6, 10 mM), and the  $\lambda_{\max}$  was 553.2 nm. With the addition of L-His, the target molecules were adsorbed in the MIPH, making the  $\lambda_{\max}$  move to the long wavelength direction own to the increase of  $n_{\text{eff}}$ .

### The effect of imprinted conditions on the Bragg diffraction peak

The mixing solvent of methanol and water was selected to make all the ingredients fully mixing. The response behavior of hydrogel can be influenced by changed the proportion of methanol and water. The methanol can make all the ingredients into one phase and facilitate the formation of the pore structure in the polymer hydrogel. In addition, the water has the vital role in preparing the aqueous phase molecularly imprinted hydrogel. However, the high polarity of water may be a disadvantage for the formation of hydrogen bond between the MAA and L-His [35]. Thus, the mixing solvent of water-methanol (1:2, V/V) can ensure good recognition ability of imprinted hydrogel and a tolerable solubility of polymerization solution.

The carboxyl groups in MIPH will protonate in a high acidity, which reduce the osmotic pressure of the hydrogel, further leading the MIPH shrinking and making the diffraction wavelength blue-shifted. The experimental results show that the Bragg diffraction peak of the MIPH appears at 552.3 nm under pH 7.6, and it appears at 535.1 nm under pH 6.5. This illustrates that the shifts of Bragg diffraction peak of the MIPH decrease with the increase of acidity. Such a phenomenon may weaken the responsiveness of hydrogel to L-His molecules. On the other hand, the osmotic pressure of hydrogel is increased in the low ionic strength solutions, which can lead to a swell of MIPH and make the Bragg diffraction peak red-shift [34], it also weaken the sensing sensitivity of the MIPH sensor. Therefore, the phosphate buffer (pH 7.6, 10 mM) was determined to provide favorable environment for the detection of target molecules.

In addition, MAA can combine reversibly with L-His through non-covalent interactions, and EGDMA is used as the cross-linker due to its beneficial to the synthesis of polymer. The ratio of monomer and cross-linker has great influence on the structure and strength of MIPH. In order to improve the recognition capability of imprinted hydrogel, several control experiments have been conducted by adjusting the proportion of monomer and cross-linker. The ratio of MAA:EGDMA were chosen as (a) 14:2.5, (b) 14:3, (c) 14:3.5 for the experiment conditions respectively. And their recognition abilities for L-His molecules were investigated in buffer solution with different concentrations of L-His.

As shown in Fig. 3, the diffraction wavelengths of all MIPHs have some redshifts with increasing of L-His, but the amount of the shifts decreases with increasing the proportion of cross-linker. Such a result means the recognition capacity of hydrogel for target molecule is weakened under the high

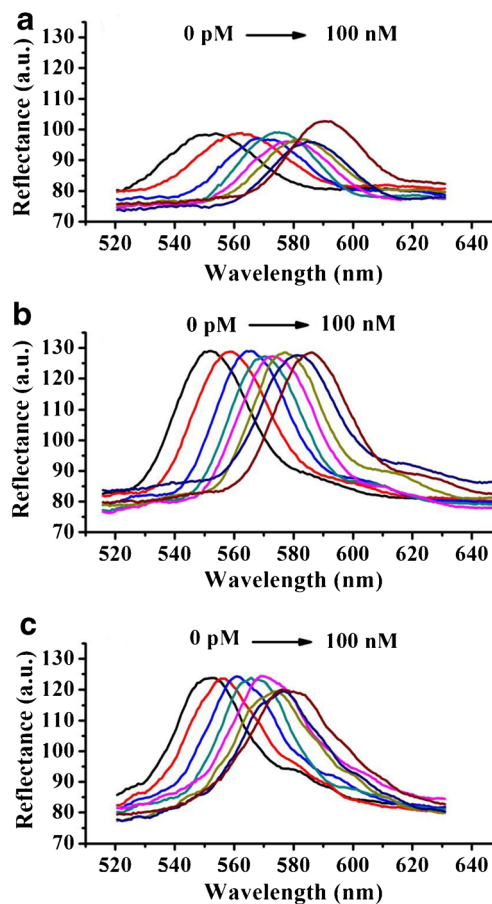


**Fig. 3** The Bragg diffraction peaks of MIPH film with different ratios of monomer and cross-linker in a series of concentrations of L-His solution (0 pM, 10 pM, 100 pM, 1 nM, 5 nM, 10 nM, 50 nM, 100 nM). The ratio of MAA:EGDMA is **a** 14:2.5, **b** 14:3, and **c** 14:3.5, respectively

content of EGDMA. While the ratio of MAA:EGDMA is 14:2.5 (Fig. 3a), the diffraction peaks are irregular due to the poor intensity of hydrogel. On the other hand, under the high content of cross-linker like 14:3.5 (Fig. 3c), the redshifts of this MIPH are lesser than those with low cross-linker content. These can be explained that the high content of cross-linker can keep the integrity of the structure and obtain highly ordered nano-cavities. However, it makes the MIPH difficult to release and absorb the L-His molecules. Contrarily, the low content of cross-linker can enhance the elasticity of hydrogel but reduce the intensity of the Bragg diffraction peak. And while the ratio is 14:3, the MIPH exhibit good physical strength and obvious shifts in the diffraction peak. Consequently, the MAA:EGDMA is 14:3 can bring good responsiveness ability for MIPH.

### Optical response of the imprinted and non-imprinted photonic hydrogel to L-His

The optical sensing performance of the MIPH was investigated by immersing the hydrogel into the L-His solutions with

different concentrations. The L-His molecules can combine with the specific nano-cavities, which increase the average refractive index of the MIPH, and lead to a redshift of the Bragg diffraction peak. As shown in Fig. 3b, the maximum Bragg diffraction peak of the MIPH appears at 552.3 nm in the blank phosphate buffer, and it is gradually red-shifted with the increasing of the L-His. The shift of the diffraction peak reaches at 34.1 nm ( $\lambda_{\max} = 586.4$  nm) in 100 nM L-His solution, and there is still a response signal of the diffraction peak shift (5.8 nm) when the concentration of L-His is low to 10 pM. These experimental results demonstrate that the MIPH sensor can sensitively detect the L-His molecules.

In order to further understand the identification properties of the molecularly imprinted hydrogel materials, the non-molecularly imprinted photonic hydrogel (NIPH) has been prepared. This control-experiment was performed under the same preparation conditions of the MIPH only without addition of L-His. As shown in Fig. 4, without specific recognition sites, there is no significant shift in the Bragg diffraction peaks under the different concentrations of L-His. This illustrates that the specific binding behavior between the porous sites and the target molecules provide a good recognition ability and optical signal for MIPH. Moreover, the diffraction peaks of NIPH appear at the longer wavelength region than those of the MIPH. This is due to the absence of target molecularly imprinted cavities usually leading an increase in the average effective refraction, making the Bragg diffraction red-shift according to Bragg Eq. (1).

### Selectivity and selectivity of the MIPH

The specific recognition ability of MIPH mainly depends on two factors. One is the structure of target molecules that matches the imprinted cavities. The other is the hydrogen bonding between the target molecules and the functional groups of the MIPH. To investigate the selectivity of this sensor, several experiments were conducted by testing the responses of MIPH to D-Histidine, Histamine, Cysteine, Glycine, Lysine,

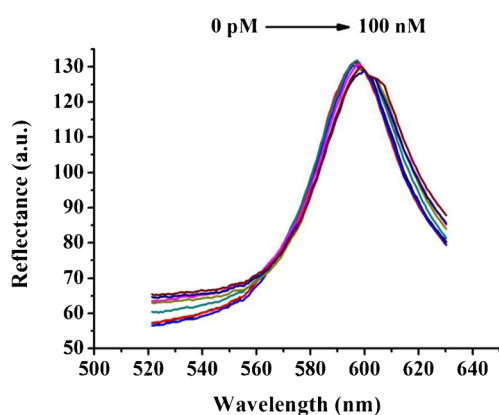


**Fig. 4** The Bragg diffraction peaks of the non-imprinted (NIPH) film in different concentrations of L-His solution (0 pM, 10 pM, 100 pM, 1 nM, 5 nM, 10 nM, 50 nM, 100 nM)

Tryptophan, Tyrosine and L-Phenylalanine form 10 pM to 100 nM in phosphate buffer. The shifts of the Bragg diffraction peaks of MIPH for these are shown in Fig. 5a. It can be seen that the MIPH has no significant response for neither the simple amino acids (e.g. Glycine) nor the complex amino acids which containing the benzene ring (e.g. L-Phenylalanine). And the testing in D-His shows the MIPH has chiral recognition to a certain extent. In addition, a mix sample contains 100 nM of Histamine, D-His and L-His was tested. The result is shown in Fig. 5b, which is similar to the test in 100 nM L-His, and showing an anti-interference ability to MIPH. These experimental results clearly illustrate that only L-His molecules can combine with the imprinted cavities and lead to a redshift in the Bragg diffraction peak. Furthermore, due to the weak nonspecific adsorption of MIPH for small molecules, there still have slight responses for other amino acids.

### Response speed and recoverability of MIPH

The inverse opal photonic crystals have large porous structure. This warrants low mass diffusion resistance and high specific surface, making target molecules quickly reach to the recognition sites. In addition, the high affinity between the target molecules and the recognition sites can also accelerate the diffusion of the L-His. The above factors can shorten the response time of the sensor. As shown in Fig. 6a, the adsorption

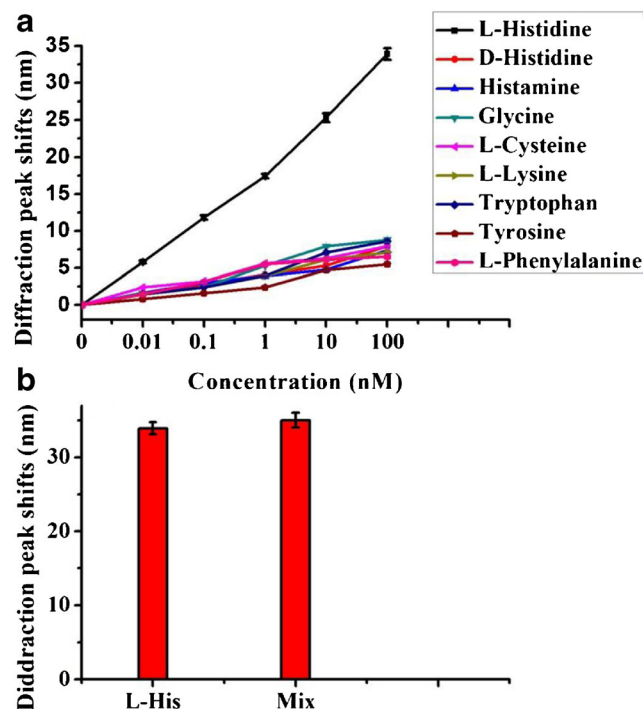


**Fig. 5** **a** The selective experiment of MIPH in different concentration of analytes. **b** The anti-interference experiment of the MIPH sensor (the mix sample contains 100 nM of Histamine, D-His and L-His). The error bars indicate the deviation for three assays

of hydrogel to L-His can be achieved within about 60 s, showing a rapid response ability of the MIPH.

Furthermore, the MIPH has good mechanical strength and chemical stability due to the proper proportion of cross-linker and functional monomer. The target molecules that have bonded to the MIPH can be eluted by rinsing with 0.1 M acetic acid. After immersing in blank phosphate buffer, the MIPH is easily recovered to the initial state. Figure 6b indicates the maximum diffraction wavelength of imprinted hydrogel under 10 nM L-His solution for five cycles. The result shows that the relative deviation of the shifts of maximum diffraction wavelength is less than 3%, which illustrates that the MIPH has good recoverability in detecting L-His. In addition, the sensor still has good response ability after placement for a month, indicative of the MIPH has excellent stability.

### Adsorption capacity of the inverse opal photonic crystals (MIPH)

The Scatchard analysis was applied to investigate the adsorption capacity of the MIPH for L-His and it follows the Scatchard equation at equilibrium:

$$\frac{Q}{C} = \frac{Q_M - Q}{k_D} \tag{3}$$

In which Q is the amount of binding L-His,  $Q_M$  ( $\mu\text{mol/g}$ ) is the amount of apparent maximum adsorption of L-His, C is

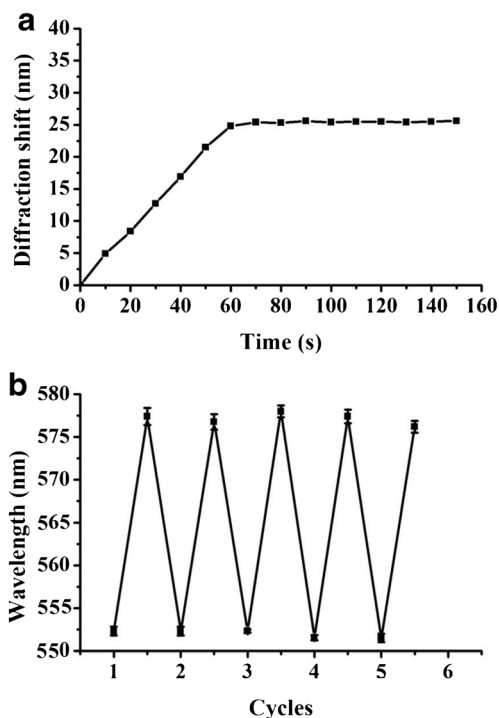


**Fig. 6** a The kinetic response of MIPH to L-His in 10 nM. b The maximum diffraction wavelength of the MIPH under 10 nM L-His with five cycles. The error bars indicate the deviation for three assays

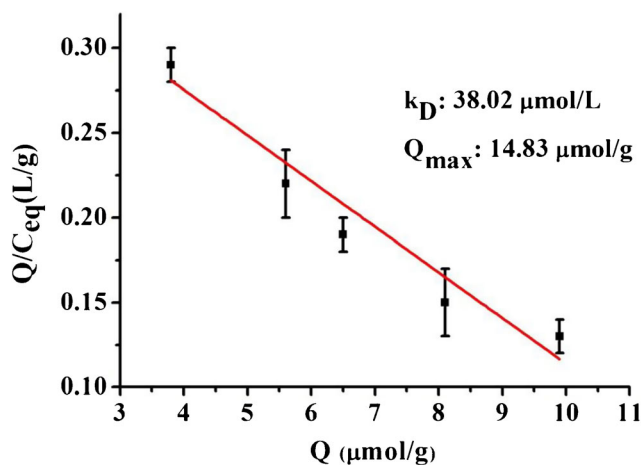


**Fig. 7** The Scatchard analysis is used to analyze the adsorption capacity of MIPH to L-His. The error bars indicate the deviation for three assays

the concentration of L-His at equilibrium and  $k_D$  ( $\mu\text{mol/L}$ ) is the equilibrium dissociation constant. Figure 7 shows the Scatchard plot is linear, which indicates that only one kind of binding site in this MIPH. And the MIPH has a  $Q_M$  of  $14.83 \mu\text{mol/g}$  and  $k_D$  of  $38.02 \mu\text{mol/L}$  to L-His.

### Analytical application to drinks sample

In order to evaluate the practical application of the MIPH, the sensor was applied to analyze L-His in drinks sample. The shifts of diffraction wavelength of the MIPH were recorded after the MIPH was stable in the sample solutions, and the results are shown in Fig. 8. The redshifts of diffraction wavelength can be found in the test of drinks sample, and the values of shift are similar with those in phosphate buffer. Its indicates that the MIPH has a good sensitive response to L-His in drinks with existence of interference, showing this MIPH method has a good potential application.

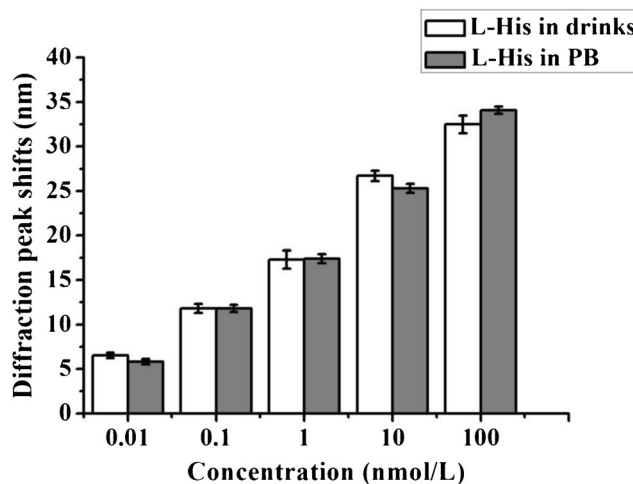


**Fig. 8** To analysis the response capability of the MIPH film to L-His in drinks and phosphate buffer. The error bars indicate the deviation for three assays

## Conclusion

A molecularly imprinted photonic hydrogel sensor has been developed for detection of L-His. By combining the indicative function of photonic crystals with the specific recognition ability of molecular imprinting, this MIPH sensor can directly generate an optical signal after identifying L-His without adding any chemical or biological modifications. In addition, the MIPH has good sensitive response in drinks sample, and the response can be completed in 60 s, which suggests it can become a fast screening method to detect L-His. However, one of the challenge of the method is that it is not easy to show an accurate quantitative equation to describe the relationship between the diffraction shift and the concentration of L-His. And the other one is that the ion strength and pH can influence the detection capability of MIPH in a certain range. In order to get the accurate measurement results, the ion strength and pH need to be controlled. After solving these problems, it will provide a great potential detection technique for L-His in the future.

**Acknowledgements** This study was financially supported by the National Natural Science Foundation of China (21874037, 21675045, and 21505038) and the International Scientific and Technological Cooperation Projects of China (2012DFR40480).

**Compliance with ethical standards** This article does not contain any studies with human participants or animals performed by any of the authors. In this experiment, we did not collect any samples of human and animals.

## References

- Nan CG, Ping WX, Ping DJ, Qing CH (1999) A study on electrochemistry of histidine and its metabolites based on the diazo coupling reaction. *Talanta* 49(2):319–330
- Rawat KA, Kailasa SK (2014) Visual detection of arginine, histidine and lysine using quercetin-functionalized gold nanoparticles. *Microchim Acta* 181(15–16):1917–1929
- Yu M, Chu W, Wu Z (2010) XAFS study of the configuration of l-histidine with Mn<sup>2+</sup>, Co<sup>2+</sup>, Ni<sup>2+</sup>, Cu<sup>2+</sup>, Zn<sup>2+</sup> at pH 6.0. *Nucl Inst Methods Phys Res A* 619(1):408–410
- Sasmal M, Maiti TK, Bhattacharyya TK (2015) Ultra-low level detection of L-histidine using solution-processed ZnO nanorod on flexible substrate. *IEEE Trans Nanobiosci* 14(6):634–640
- Meng J, Zhang W, Cao C-X, Fan L-Y, Wu J, Wang Q-L (2010) Moving affinity boundary electrophoresis and its selective isolation of histidine in urine. *Analyst* 135(7):1592–1599
- Wadud S, Or-Rashid MM, Onodera R (2002) Method for determination of histidine in tissues by isocratic high-performance liquid chromatography and its application to the measurement of histidinol dehydrogenase activity in six cattle organs. *J Chromatogr B* 767(2):369–374
- Zheng X, Yao T, Zhu Y, Shi S (2015) Cu(2+) modulated silver nanoclusters as an on-off-on fluorescence probe for the selective detection of L-histidine. *Biosens Bioelectron* 66:103–108
- Shamsipur M, Molaabasi F, Shanehsaz M, Moosavi-Movahedi AA (2015) Novel blue-emitting gold nanoclusters confined in human hemoglobin, and their use as fluorescent probes for copper(II) and histidine. *Microchim Acta* 182(5–6):1131–1141
- Zhu X, Zhao T, Nie Z, Miao Z, Liu Y, Yao S (2016) Nitrogen-doped carbon nanoparticle modulated turn-on fluorescent probes for histidine detection and its imaging in living cells. *Nanoscale* 8(4):2205–2211
- Li L-D, Chen Z-B, Zhao H-T, Guo L (2011) Electrochemical real-time detection of l-histidine via self-cleavage of DNAzymes. *Biosens Bioelectron* 26(5):2781–2785
- Chen Z, Nai J, Ma H, Li Z (2014) Nickel hydroxide nanocrystals-modified glassy carbon electrodes for sensitive l-histidine detection. *Electrochim Acta* 116:258–262
- Natsume T, Nakayama H, Cs J, Isobe T, Takio K, Mikoshiba K (2000) Combination of biomolecular interaction analysis and mass spectrometric amino acid sequencing. *Anal Chem* 72(17):4193–4198
- Yablonovitch E (1987) Inhibited spontaneous emission in solid-state physics and electronics. *Phys Rev Lett* 58(20):2059–2062
- John S (1987) Strong localization of photons in certain disordered dielectric superlattices. *Phys Rev Lett* 58(23):2486–2489
- Fenzl C, Hirsch T, Wolfbeis OS (2014) Photonic crystals for chemical sensing and biosensing. *Angew Chem Int Ed* 53(13):3318–3335
- Lee K, Asher SA (2000) Photonic crystal chemical sensors: pH and ionic strength. *J Am Chem Soc* 122(39):9534–9537
- Wang J, Cao Y, Feng Y, Yin F, Gao J (2007) Multiresponsive inverse-opal hydrogels. *Adv Mater* 19(22):3865–3871
- Ye B, Zhao Y, Cheng Y, Li T, Xie Z, Zhao X, Gu Z (2012) Colorimetric photonic hydrogel aptasensor for the screening of heavy metal ions. *Nanoscale* 4(19):5998–6003
- Xue F, Meng Z, Wang F, Wang Q, Xue M, Xu Z (2014) A 2-D photonic crystal hydrogel for selective sensing of glucose. *J Mater Chem* 2(25):9559–9565
- Hu X, Li G, Li M, Huang J, Li Y, Gao Y, Zhang Y (2008) Ultrasensitive specific stimulant assay based on molecularly imprinted photonic hydrogels. *Adv Funct Mater* 18(4):575–583
- Wang C, Lim CY, Choi E, Park Y, Park J (2016) Highly sensitive user friendly thrombin detection using emission light guidance from quantum dots-aptamer beacons in 3-dimensional photonic crystal. *Sensors Actuators B Chem* 223:372–378
- Wulff G (2002) Enzyme-like catalysis by molecularly imprinted polymers. *Chem Rev* 102(1):1–27
- Wackerlig J, Lieberzeit PA (2015) Molecularly imprinted polymer nanoparticles in chemical sensing – synthesis, characterisation and application. *Sensors Actuators B Chem* 207:144–157
- Cheong WJ, Yang SH, Ali F (2013) Molecular imprinted polymers for separation science: a review of reviews. *J Sep Sci* 36(3):609–628
- Schirhagl R (2014) Bioapplications for molecularly imprinted polymers. *Anal Chem* 86(1):250–261
- Wang H, Yi J, Velado D, Yu Y, Zhou S (2015) Immobilization of carbon dots in molecularly imprinted microgels for optical sensing of glucose at physiological pH. *ACS Appl Mater Interfaces* 7(29):15735–15745
- Kamra T, Zhou T, Montelius L, Schnadt J, Ye L (2015) Implementation of molecularly imprinted polymer beads for surface enhanced Raman detection. *Anal Chem* 87(10):5056–5061
- Wei C, Zhou H, Zhou J (2011) Ultrasensitively sensing acetate using molecular imprinting techniques on a surface plasmon resonance sensor. *Talanta* 83(5):1422–1427
- Li N, Qi L, Shen Y, Qiao J, Chen Y (2014) Novel oligo(ethylene glycol)-based molecularly imprinted magnetic nanoparticles for thermally modulated capture and release of lysozyme. *ACS Appl Mater Interfaces* 6(19):17289–17295
- Chen L, Xu S, Li J (2011) Recent advances in molecular imprinting technology: current status, challenges and highlighted applications. *Chem Soc Rev* 40(5):2922–2942



31. Lofgreen JE, Ozin GA (2014) Controlling morphology and porosity to improve performance of molecularly imprinted sol-gel silica. *Chem Soc Rev* 43(3):911–933
32. Guo C, Zhou C, Sai N, Ning B, Liu M, Chen H, Gao Z (2012) Detection of bisphenol a using an opal photonic crystal sensor. *Sensors Actuators B Chem* 166-167:17–23
33. Hu X, An Q, Li G, Tao S, Liu J (2006) Imprinted photonic polymers for chiral recognition. *Angew Chem Int Ed* 45(48):8145–8148
34. Meng L, Meng P, Zhang Q, Wang Y (2013) Fast screening of ketamine in biological samples based on molecularly imprinted photonic hydrogels. *Anal Chim Acta* 771:86–94
35. Jiang P, Hwang KS, Mittleman DM, Bertone JF, Colvin VL (1999) Template-directed preparation of macroporous polymers with oriented and crystalline arrays of voids. *J Am Chem Soc* 121(50): 11630–11637